

HUBBLE ULTRA DEEP FIELD–JD2: MID-INFRARED EVIDENCE FOR A $z \sim 2$ LUMINOUS INFRARED GALAXY

RANGA-RAM CHARY,¹ HARRY I. TEPLITZ,¹ MARK E. DICKINSON,² DAVID C. KOO,³ EMERIC LE FLOC’H,^{4,5}
DELPHINE MARCILLAC,⁶ CASEY PAPOVICH,^{5,6} AND DANIEL STERN⁷

Received 2007 February 1; accepted 2007 April 25

ABSTRACT

The Hubble Ultra Deep Field source JD2 presented in Mobasher et al. is an unusual galaxy that is very faint at all wavelengths shortward of $1.1 \mu\text{m}$. Photometric redshift fits to data between 0.4 and $8 \mu\text{m}$ yield a significant probability that it is an extremely massive galaxy at $z \sim 6.5$. In this paper we present new photometry at 16 and $22 \mu\text{m}$ from *Spitzer* Infrared Spectrograph (IRS) peak-up imaging of the Great Observatories Origins Deep Survey (GOODS) fields. We find that the spectral energy distribution shows a factor of ~ 4 rise in flux density between the 16 and $22 \mu\text{m}$ bandpass, which is most likely due to the entrance of polycyclic aromatic hydrocarbon emission features into the 22 and $24 \mu\text{m}$ passbands. The flux ratio between these bandpasses can be best fit by a $z = 1.7$ luminous infrared galaxy with a bolometric luminosity of $(2\text{--}6) \times 10^{11} L_{\odot}$ corresponding to a star formation rate of $80 M_{\odot} \text{yr}^{-1}$. The predicted flux density values at other longer wavelengths are below the detection limits of current instrumentation, but such sources could potentially be detected in lensed submillimeter surveys. Reevaluation of the optical/near-infrared photometry continues to favor $z > 6$ photometric redshift solutions, but we argue that the consistency of the multi-wavelength parameters of this galaxy with other dusty starbursts favor the $z \sim 2$ mid-infrared photometric redshift. The data presented here provide evidence that optically undetected near-infrared sources that are detected at $24 \mu\text{m}$ are most likely dusty, starburst galaxies at a redshift of $z \sim 2$ with stellar masses $> 10^{10} M_{\odot}$.

Subject headings: cosmology: observations — early universe — galaxies: evolution — galaxies: individual (HUDF-JD2)

1. INTRODUCTION

JD2 is an interesting object in the Hubble Ultra Deep Field (UDF; Thompson et al. 2005; Beckwith et al. 2006). Its non-detection shortward of the $1.1 \mu\text{m}$ bandpass, even in ultradeep Advanced Camera for Surveys (ACS) UDF optical data that are sensitive down to ~ 29 AB magnitude, has been interpreted as being due to the redshifted Lyman break. In addition, it displays a break in its broadband spectral energy distribution (SED) between 2.2 and $3.6 \mu\text{m}$, which has been interpreted as the redshifted Balmer break. Mobasher et al. (2005) argue that it may be a very massive ($6 \times 10^{11} M_{\odot}$) galaxy with very little ongoing star formation at $z \sim 6.5$. The large stellar mass of this galaxy derived from fitting population synthesis models to the multiband photometry, and high source density implied by the presence of one such object in the small area subtended by the Near-Infrared Camera and Multi-Object Spectrograph (NICMOS) UDF, suggest that ultraviolet-faint objects, if indeed at such high redshifts, contribute as much to the stellar mass density at $z \sim 6.5$ as rest-frame ultraviolet-bright Lyman break galaxies. Since the age of the stellar population in JD2 is thought to be ~ 600 Myr, galaxies like JD2 might harbor remnants of the first epoch of star formation, and play an important role in the reionization of the intergalactic medium (IGM). Such an object, if truly at high redshift, would challenge current models of galaxy formation, which do not predict a large number

density of galaxies more massive than $10^{11} M_{\odot}$ at $z > 6$ (Davé et al. 2006).

The photometric redshift solutions in Mobasher et al. (2005) favor a $z \approx 6.5$ solution but provide a 15% probability that the source is at $z < 5$, with the most likely alternative solution implying a dusty galaxy at $z \approx 2.5$. There are a few inconsistencies in the high-redshift interpretation of JD2. The optical/near-infrared SED is best fit by a template without significant extinction or star formation. However, the object is detected in the Great Observatories Origins Deep Survey (GOODS) *Spitzer* Multi-band Imaging Photometer and Spectrometer (MIPS) $24 \mu\text{m}$ survey with a flux density of $51.4 \pm 4 \mu\text{Jy}$. Since the $24 \mu\text{m}$ flux would be dominated by redshifted hot dust and polycyclic aromatic hydrocarbon (PAH) emission, it indicates the presence of dust within the galaxy. The age-extinction degeneracy is very well known for red galaxies. Most recently, Stern et al. (2006) have shown that the optical/near-infrared photometry of dusty, extremely red objects (EROs) is almost identical to that of evolved, passive EROs, and that only the detection of reprocessed emission at mid- and far-infrared wavelengths can break the degeneracy. Nevertheless, Mobasher et al. (2005) suggest that the $24 \mu\text{m}$ emission could be explained by the presence of an obscured active nucleus. While this is possible, at $z \sim 6.5$, the *Chandra* 2–8 keV band traces 15–60 keV emission, energies that are relatively immune to absorption. The *Chandra* detection limit corresponds to L_X of $3 \times 10^{43} \text{ ergs s}^{-1}$ at $z = 6.5$, while the mid-infrared detection implies νL_{ν} at rest $3 \mu\text{m}$ of $3 \times 10^{45} \text{ ergs s}^{-1}$. The $10 \mu\text{m}$ to X-ray luminosity ratios of local Seyfert nuclei are ~ 3 (e.g., Krabbe et al. 2001), and the flat spectrum of Seyferts in νL_{ν} , implies that either large ($N_{\text{H}} \gg 10^{24} \text{ cm}^{-2}$) column densities of neutral gas must be obscuring the hard X-ray emission, or the active galactic nucleus (AGN) is an unusually low luminosity X-ray source.

¹ *Spitzer* Science Center, California Institute of Technology, Pasadena, CA 91125; rchary@caltech.edu.

² National Optical Astronomy Observatory, Tucson, AZ 85719.

³ UCO/Lick Observatory, University of California, Santa Cruz, CA 95064.

⁴ Institute for Astronomy, Honolulu, HI 96822.

⁵ *Spitzer* Fellow.

⁶ Steward Observatory, University of Arizona, Tucson, AZ 85721.

⁷ Jet Propulsion Laboratory, Pasadena, CA 91109.

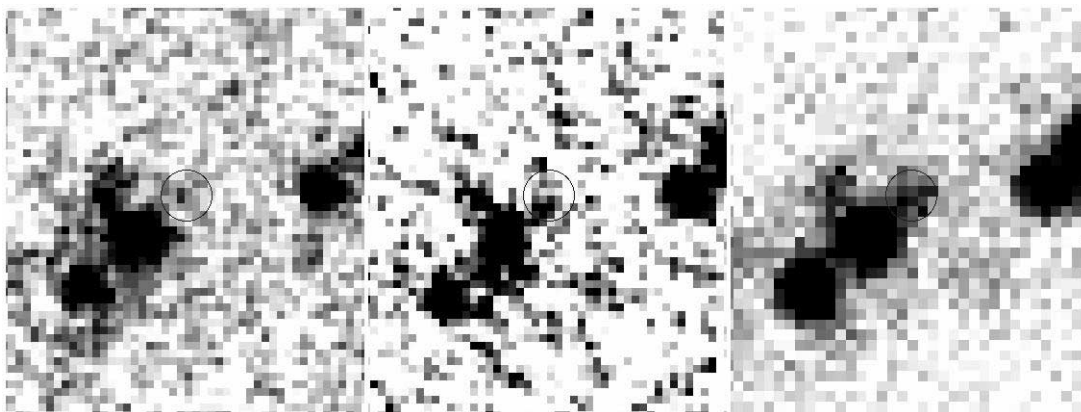


FIG. 1.—16, 22, and 24 μm snapshots of the Hubble Ultra Deep Field source JD2 (circled) illustrating the quality of *Spitzer* mid-infrared data on this source. Images are $\sim 40''$ on a side, with north up and east to the left. JD2 is at $3^{\text{h}}32^{\text{m}}38.74^{\text{s}}$, $-27^{\circ}48'39.9''$ (J2000.0).

In a recent paper, Dunlop et al. (2007) question the optical limits in the B , V , i , and z passbands adopted by Mobasher et al. (2005) and demonstrate that the χ^2 values in the redshift fits are skewed in the Mobasher et al. (2005) analysis by adopting optical flux limits that are too stringent. By refitting the source with revised optical limits, they conclude the source to be at $z \sim 2.2$ rather than at $z \sim 6.5$. We also note that JD2 has been visited in work by Yan et al. (2004) and Chen & Marzke (2004) prior to the Mobasher et al. (2005) analysis, and had been classified as a $z \sim 3$ ERO.

In this paper, we present new 16 and 22 μm photometry of this source from *Spitzer* Infrared Spectrograph (IRS) peak-up imaging of the GOODS fields (Teplitz et al. 2006). We fit the photometry at these two wavelengths and the published 24 μm data with a variety of dust SEDs and demonstrate that the mid-infrared photometry is most consistent with a redshift of $z \sim 1.7$ for JD2. We assess the accuracy of the optical/near-infrared photometry and refit the data with this redshift constraint to determine physical properties of the galaxy. We conclude that it is a luminous infrared galaxy (LIRG) with $L_{\text{IR}} \sim 10^{11.7} L_{\odot}$ and not a $z > 6$ galaxy with a dust-obscured AGN. Throughout this paper, we adopt a $\Omega_M = 0.27$, $\Omega_{\Lambda} = 0.73$, $H_0 = 71 \text{ km s}^{-1} \text{ Mpc}^{-1}$ cosmology.

2. IRS PEAK-UP IMAGING OF GOODS-S

The 16 and 22 μm observations were carried out using the peak-up imaging capability of the Infrared Spectrograph (IRS) instrument (Houck et al. 2004) on the *Spitzer Space Telescope*. The field of view of the peak-up imaging camera is $54'' \times 80''$. The central $\sim 130 \text{ arcmin}^2$ of the GOODS-S field was observed with 60 s frame times. Most of the area within the GOODS fields had four dithers per position, while the UDF area had 32 dithers per position. Each frame was distortion corrected and background subtracted. The dithered frames were combined using “drizzle” (Fruchter & Hook 2002). Due to the limited number of dithers per position, point kernel drizzling, which would have minimized the correlated noise in the mosaics, was not possible. The final mosaics have a plate scale of $0.9'' \text{ pixel}^{-1}$. The exposure time in the final mosaics is $\sim 4 \text{ minutes pixel}^{-1}$ over most of the GOODS area, while the UDF area was observed with 32 minutes pixel^{-1} . JD2, although in the UDF region, serendipitously lies in a part of the coverage map where the exposure time is 68 minutes, about twice that of the nominal UDF. As a result, the statistical uncertainty on its flux is lower than for the average UDF source of the same brightness.

The spatial resolution of *Spitzer* at 16 and 22 μm is $4.1''$ and $5.2''$ full width at half-maximum (FWHM), respectively. At this resolution, the majority of sources, including JD2, are point sources. This makes it possible to use prior positions from higher resolution data, such as the GOODS 3.6–8 μm imaging (Dickinson et al. 2003; M. Dickinson et al. 2007, in preparation) and apply point-source fitting techniques to measure the flux density of the source. The technique has successfully been used for cataloging 24 μm sources from the GOODS MIPS imaging survey. The results are consistent with aperture photometry, with appropriate aperture corrections, for isolated sources, and alleviate the contamination to the photometry from the wings of the point-spread function for sources that have nearby companions. Postage stamp image cutouts of JD2 are shown in Figure 1.

The 16 and 22 μm flux densities of the source are 13.5 ± 3.5 and $56 \pm 12 \mu\text{Jy}$, respectively. In comparison, the 24 μm flux density of the source from the GOODS imaging of the field is $51 \pm 4 \mu\text{Jy}$. Hubble Ultra Deep Field source JD2 (HUDF-JD2) is separated by $7''$ from a brighter mid-infrared source to the southeast, which is a $z = 0.457$ spiral galaxy (D. Stern et al. 2007, in preparation). In order to estimate the systematic uncertainty associated with fitting the flux density of a faint source near a bright one, we performed a Monte Carlo simulation. We identified a relatively isolated source in the mosaic with about the same flux density as the spiral galaxy: this is the galaxy at $3^{\text{h}}32^{\text{m}}43.49^{\text{s}}$, $-27^{\circ}45'56.45''$ (J2000.0), which has a flux density of $121 \pm 10 \mu\text{Jy}$ at 16 μm . We added an artificial source at a distance between $7''$ and $8''$ from this source and extracted the flux density using the positional priors. The process was repeated 100 times each for a range of flux densities straddling the measured flux density of the source. The extracted flux was compared with the input flux density to assess the systematic uncertainty and/or flux bias in the measurement. For a source with a brightness comparable to JD2, the Monte Carlo analysis yielded 1σ uncertainties of 14, 12, and $10 \mu\text{Jy}$ at 16, 22, and 24 μm , respectively. This systematic uncertainty is primarily due to the extended wings of the brighter source and is a factor of ~ 2 – 3 larger than the statistical uncertainty. We therefore adopt values of $14 \pm 14 \mu\text{Jy}$ at 16 μm , $56 \pm 12 \mu\text{Jy}$ at 22 μm , and $51 \pm 10 \mu\text{Jy}$ at 24 μm for JD2.

The sharp increase in flux density between 16 and 22 μm can either be due to the entrance of PAHs into the 22 and 24 μm bandpasses or the 9.7 μm silicate absorption feature entering the 16 μm bandpass. A third possibility is the decreasing contribution from hot dust surrounding an AGN because the dust is close

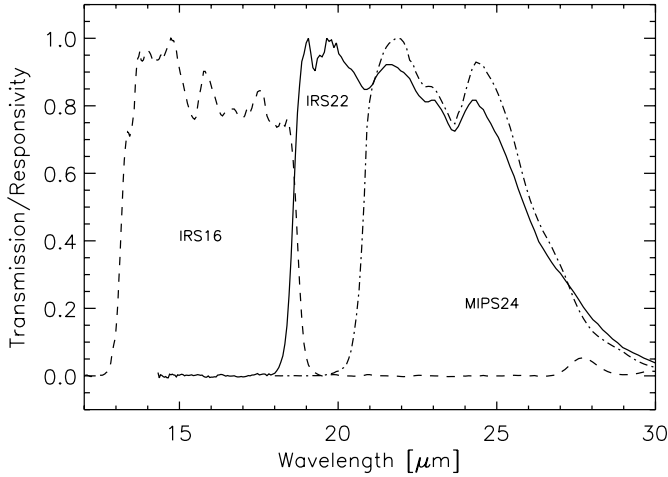


FIG. 2.—Response curves for the IRS 16 and 22 μm bandpasses, and MIPS 24 μm bandpass.

to its sublimation temperature. We evaluate each of these possibilities in the following sections.

We note that the IRS is calibrated with respect to a constant νF_ν source spectrum. Color-correction terms to the observed flux are smaller than 1% for the 16 and 22 μm data for the observed source spectrum and can be neglected. Furthermore, when we estimate fits to the observed photometry, we integrate template spectra over the filter bandpasses (Fig. 2).

3. DERIVED SOURCE PARAMETERS

The optical/near-infrared photometry of JD2 has been discussed in Mobasher et al. (2005) and Dunlop et al. (2007). SED fits to the photometry, which provide a photometric redshift solution, show a bimodal distribution of minimum χ^2 values at $z \sim 2.5$ and $z \sim 6.5$. One set of χ^2 values are favored over the other depending on the choice of optical photometry. Mobasher et al. (2005), with their stringent $B\text{V}z$ limits, derive the proba-

bility of a $z < 5$ source to be 15%. Dunlop et al. (2007) instead adopt marginal detections of the source in the Viz bandpasses, which we discuss in § 3.2. Any significant detection of the galaxy at optical wavelengths would rule out a photometric redshift solution that favors $z > 6$. Dunlop et al. (2007) find a minimum in the χ^2 distribution at $z \sim 2.2$.

The detection of HUDF-JD2 in the deep GOODS 24 μm images did not break the degeneracy. Mobasher et al. (2005) suggest the hot dust emission is from an obscured AGN in the galaxy. Alternately, the 24 μm emission could be dominated from PAH features that would be present if the object is an extremely red, dusty starburst galaxy at $z \sim 2.5$ (Yan et al. 2004; Stern et al. 2006). Inclusion of the 16 and 22 μm data allows us to measure a photometric redshift from the mid-infrared that could potentially break this degeneracy, independent of the optical/near-infrared SED fits. Although fitting optical to mid-infrared data simultaneously is more elegant, it is virtually impossible, since there is virtually no correlation between optical/near-infrared SEDs and mid-infrared SEDs of galaxies.

3.1. Mid-Infrared Photometric Redshifts

The mid-infrared SED of a star-forming galaxy is a complicated interplay of warm dust continuum, PAH emission, and silicate absorption features. The ratio of flux densities in the three abutting *Spitzer* passbands at 16, 22, and 24 μm allow redshifts of objects to be constrained as these dust features move through these filters. PAHs are only 0.5–1 μm wide, while the 9.7 μm silicate feature is 3–4 μm wide, depending on the continuum level adopted. As a result, adjacent passbands can show widely different flux density ratios as a function of redshift (Fig. 3).

At $0.2 < z < 0.6$, the 9.7 μm silicate feature enters the 16 μm bandpass, while the 22 and 24 μm bandpasses are tracing the warm dust and 11 and 12 μm PAH features. At these redshifts, sources show low 16 $\mu\text{m}/22 \mu\text{m}$ flux density ratios. At $0.6 < z < 1.2$, the 9.7 μm features move out of the 16 μm bandpass and into the 22 μm bandpass, while the 6.2 and 7.7 μm PAH features fall in the 16 μm window, boosting the 16 $\mu\text{m}/22 \mu\text{m}$

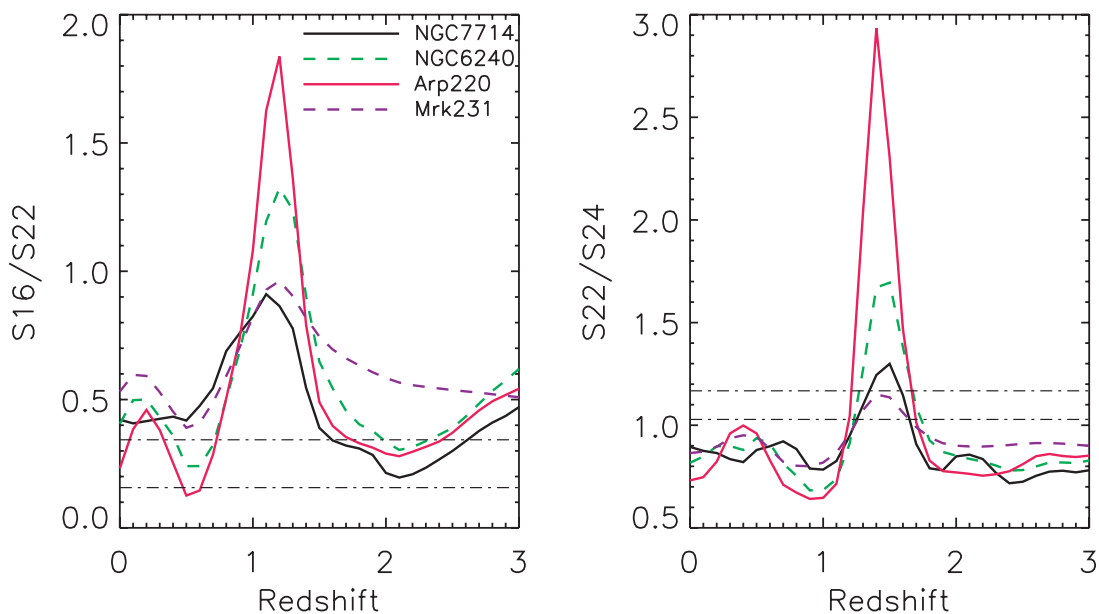


FIG. 3.—Plot of 16 $\mu\text{m}/22 \mu\text{m}$ and 22 $\mu\text{m}/24 \mu\text{m}$ flux density ratios as a function of redshift for typical infrared-luminous galaxies at $0 < z < 3$. The sources shown are NGC 7714—a typical starburst (SB) with strong PAH, NGC 6240—a composite AGN + SB object with strong PAH, Arp 220—a starburst with strong silicate absorption and weak PAH, and Mrk 231—an AGN with weak silicate absorption. The range of flux ratios of HUDF-JD2 with statistical errors is shown by the horizontal dot-dashed lines. The flux ratios indicate that JD2 is a LIRG with strong PAH at $z \sim 1.7$, or a source with strong silicate absorption at $z \sim 0.6$.

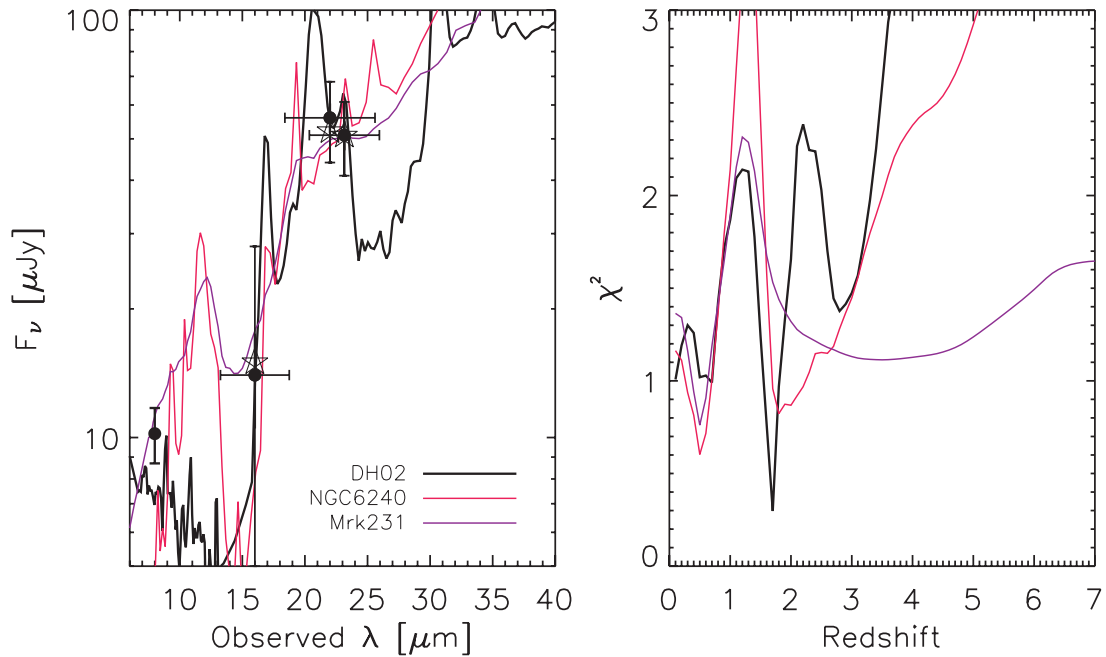


FIG. 4.—*Left*: SED fits to the mid-infrared photometry of HUDF-JD2 along with the distribution of χ^2 values with redshift (*right*). The SEDs are plotted at their best-fitting redshift, which is $z = 1.7$ for the Dale & Helou (2002) starburst templates, $z = 0.5$ for NGC 6240, and $z = 0.5$ for Mrk 231. The preferred fit (i.e., lowest χ^2 value) indicates the source is a LIRG with strong PAH emission at $z \sim 1.7$. A low χ^2 is also obtained at $z \sim 0.6$ from a source with either strong silicate absorption or the gap between the 8 and 11 μm PAH complexes. However, the $z \sim 1.7$ fit is more consistent with the fits to the optical/near-infrared photometry. The stars in the left panel are the Dale & Helou (2002) SED convolved with the filter curves.

ratio. At $1.2 < z < 1.7$, the 9.7 μm feature moves into the 24 μm band. Since the 22 μm bandpass is $\sim 2 \mu\text{m}$ wider than the MIPS 24 μm band, the 7.7 μm feature enters the 22 μm bandpass. The net effect is to boost the 22 $\mu\text{m}/24 \mu\text{m}$ flux ratio while lowering the 16 $\mu\text{m}/22 \mu\text{m}$ ratio. At $z > 1.9$, the PAH emission shifts out of the 16 μm band, decreasing the 16 $\mu\text{m}/22 \mu\text{m}$ ratio, while the 22 $\mu\text{m}/24 \mu\text{m}$ flux ratio varies as the 6.2 and 7.7 μm PAH features move within the passbands. This variation in flux ratios is illustrated in Figure 3 for four different SED types derived from spectral observations of galaxies in the local universe (Armus et al. 2007; Brandl et al. 2004).

While it is true that variation of PAH line ratios or strength of silicate absorption can cause broadband fluxes to vary significantly, the combination of photometric redshifts from the optical/near-infrared and mid-infrared photometric redshifts using these three bandpasses can help break redshift degeneracies.

The flux density ratios observed for HUDF-JD2 are a 16 $\mu\text{m}/22 \mu\text{m}$ ratio of $0.25^{+0.19}_{-0.08}$ and a 22 $\mu\text{m}/24 \mu\text{m}$ ratio of $1.1^{+0.37}_{-0.13}$. This indicates that the galaxy must either be at $z \sim 0.6$ if it has very strong silicate absorption, or at $z \sim 1.7$ if it is a typical starburst galaxy with strong PAH emission.

In Figure 4 and Table 1, we illustrate the quality of fits to the photometry at 16, 22, and 24 μm from different mid-infrared template SEDs. We consider starbursts, AGNs, and composite sources that span the range of strong PAH, weak PAH, and strong silicate absorption (Chary & Elbaz 2001; Forster-Schreiber et al. 2001; Le Floc'h et al. 2001; Dale & Helou 2002; Brandl et al. 2004; Armus et al. 2007). We also consider the nondetection of JD2 in deep 70 μm observations of the GOODS fields that achieve 5σ flux density limits of ~ 2 mJy (Frayer et al. 2006). The best fit to the 16, 22, and 24 μm photometry is from a starburst source with strong PAH emission at $z = 1.7$. The increase

TABLE 1
RESULTS OF MID-INFRARED SPECTRAL ENERGY DISTRIBUTION FITS

Template Adopted	Best-Fit Redshift	L_{IR}^{a} (L_{\odot})	χ^2	Predicted Fluxes (70, 850 μm in mJy)	Type of Object ^b	Notes
Dale & Helou.....	1.7	4.7×10^{11}	0.30	0.6, 0.5	...	
Chary & Elbaz.....	1.6	5.6×10^{11}	0.37	0.9, 0.4	...	
NGC 7714.....	1.6	2.5×10^{11}	0.42	0.4, 0.2	Starburst	
M82.....	1.7	1.6×10^{11}	0.48	0.2, 0.09	Starburst	
NGC 6240.....	0.5	1.5×10^{10}	0.60	1.0, 0.02	Compton-thick AGN + SB	Large A_V , inconsistent UV/IR SFR
Mrk 231.....	0.5	6.9×10^9	0.76	0.4, 0.004	Obscured AGN	Exceeds NIR flux
Arp 220.....	1.8	2.1×10^{12}	0.95	1.7, 1.5	Starburst	
NGC 1068–nucleus.....	3.7	1.4×10^{12}	1.02	0.3, 1.0	Obscured AGN	Worse χ^2
Mrk 231.....	6.5	7.4×10^{12}	2.0	0.2, 2.4	Obscured AGN	Worse χ^2
NGC 1068–nucleus.....	6.5	1.3×10^{13}	1.1	0.6, 7.1	Obscured AGN	Worse χ^2

^a For the star-forming templates, the star formation rate is $1.71 \times 10^{-10} L_{\text{IR}}$.

^b For the AGN templates at $z = 6.5$, the stellar photospheric emission has been subtracted from the mid-infrared photometry. To identify the best-fit mid-infrared redshift for the AGN templates the actual mid-infrared photometry was used.

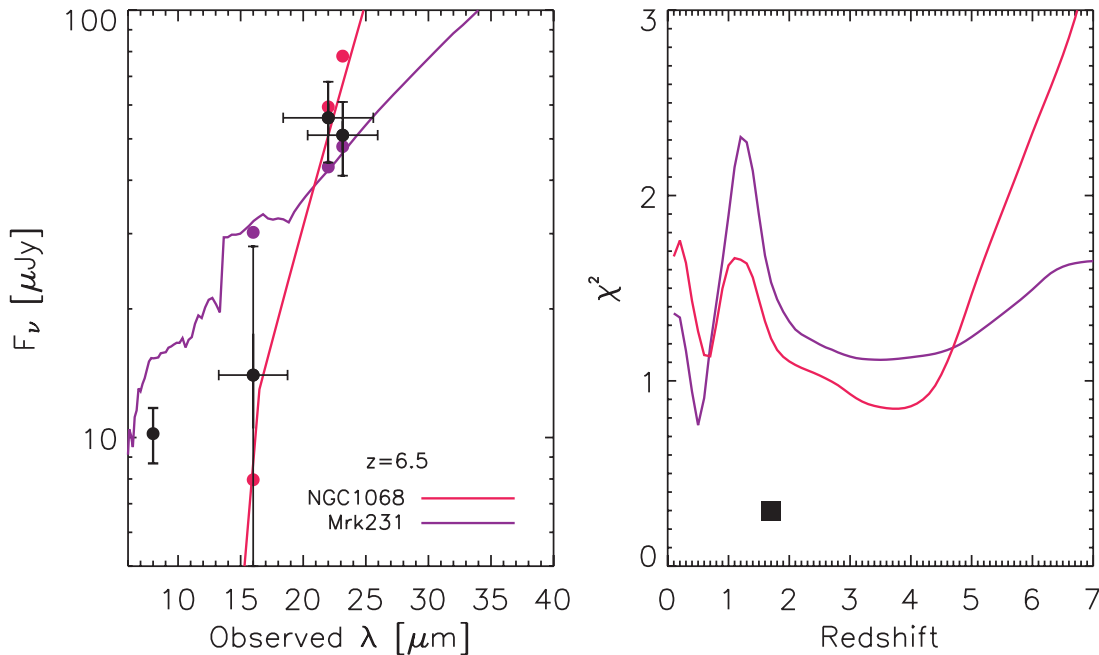


FIG. 5.—*Left:* Fits to the mid-infrared photometry of HUDF-JD2 at $z = 6.5$ using the two AGN templates presented in Mobasher et al. (2005). The filled red and purple circles are the AGN templates of the corresponding color integrated through the relevant bandpasses. The right panel shows the distribution of χ^2 values. The filled black square shows the minimum χ^2 obtained at $z = 1.7$ for the starburst SED discussed in Fig. 4 and in § 3.1. If the source were really at $z = 6.5$, there would be a stellar contribution to the mid-infrared photometry, as discussed in the text. Although this improves the formal χ^2 estimates, the $z = 6.5$ fits still yield substantially worse χ^2 estimates than the best fit at $z = 1.7$, as shown in Table 1.

in the 22 and 24 μm flux relative to 16 μm is due to the entrance of the 7.7 μm PAH complex into the 22 and 24 μm bandpasses. The flux in the 16 μm bandpass is lower, since the 6.2 μm PAH feature is much weaker.

Extrapolating the templates that are fit to the mid-infrared photometry also yields an estimate of the far-infrared (FIR) luminosity for the galaxy. The $L_{\text{IR}} = L(8\text{--}1000 \mu\text{m})$ luminosity of the source is $\sim 5 \times 10^{11} L_{\odot}$, which corresponds to a star formation rate of $80 M_{\odot} \text{yr}^{-1}$. We compare this with optical/ultraviolet estimates of star formation in § 3.3. Using the radio-FIR correlation in Yun et al. (2001) we predict the 1.4 GHz to be 12 μJy and the 8.4 GHz flux density to be 3.7 μJy , while the predicted fluxes at 70 and 850 μm are shown in Table 1. The deepest 70 and 850 μm surveys are currently sensitive to 1.5–2 mJy. The predicted intensities of JD2 are below these limits, implying that confirmation of the derived far-infrared luminosity will have to await deeper observations by *Herschel* and the Atacama Large Millimeter Array.

The χ^2 values are also reduced for an obscured AGN template at $z = 0.6$, which has the observed 16 μm flux density suppressed relative to the flux density at 22 and 24 μm due to the entrance of the 9.7 μm silicate absorption feature. An obscured AGN template like Mrk 231 can also fit the 8 μm flux density of the source, as shown in Figure 4, while the starburst template fits at $z \sim 1.7$ require the optical/near-infrared flux to be dominated by starlight (Fig. 6). The nondetection of any spectral lines in the optical/near-infrared spectroscopic data presented by Mobasher et al. (2005) as well as the difficulty in accounting for the nondetection of the source at optical wavelengths (§ 3.3) makes the $z \sim 0.6$ hypothesis unlikely. On the other hand, $z \sim 1.7$ lies within the so-called redshift desert, where the [O II] $\lambda 3727$ doublet, [O III] $\lambda 5007$ line, and $\text{H}\alpha + [\text{N II}]$ lines are all severely affected by atmospheric transmission and strong OH sky lines. Furthermore, as we discuss in § 3.3, at $z = 1.7$, the red SED of the source between 2.2 μm and IRAC 3–8 μm could be due to

the broad 1.6 μm bump in the stellar SED being in the Infrared Array Camera (IRAC) passbands.

We now consider the implications of the IRS detections to the high redshift advocated in Mobasher et al. (2005). If we adopt the hypothesis that JD2 is at $z \sim 6.5$ and the 24 μm emission is dominated by AGN light, we must first subtract the stellar contribution to the mid-infrared flux densities. We find that for the SED fit by Mobasher et al. (2005) the contribution of stellar photospheric emission to the flux densities at 16, 22, and 24 μm are 10.7, 6.5, and 6.0 μJy , respectively. We then attempt to fit the starlight-subtracted mid-infrared photometry with the two

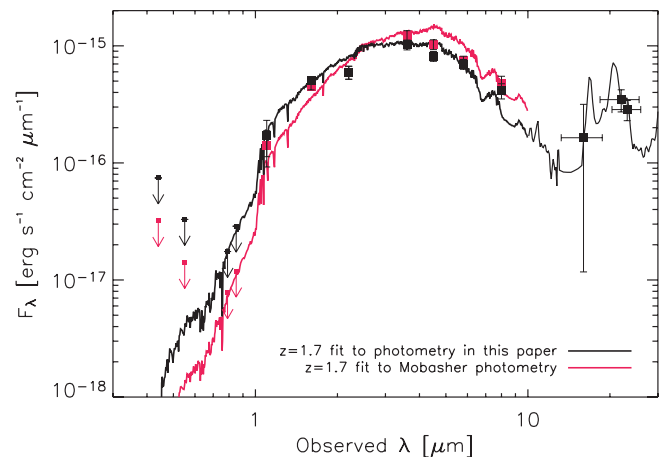


FIG. 6.—Optical to mid-infrared SED of HUDF-JD2. Filled black squares are the photometry presented in this paper. Filled red squares are the photometry in Mobasher et al. (2005). The optical/near-infrared photometry has been fit with the BC03 model, and the mid-infrared photometry has been fit with the Dale & Helou (2002) model. The source is most likely a LIRG with strong PAH emission at $z \sim 1.7$. The inferred star formation rate is $\sim 80 M_{\odot} \text{yr}^{-1}$ with ~ 4 mag of visual extinction.

mid-infrared AGN templates presented in Mobasher et al. (2005). The χ^2 values are significantly worse than the best fits at $z \sim 1.7$ (Table 1 and Fig. 5). The Mrk 231 template, fairly typical of an obscured AGN, is bluer in its $16 \mu\text{m}/22 \mu\text{m}$ flux ratios at $z = 6.5$ than the observations indicate. NGC 1068, which is a Compton-thick AGN with decreasing hot dust continuum at shorter wavelengths due to dust sublimation, would best fit the observed mid-infrared photometry at $z = 3.7$. The hot dust emission falls off too rapidly for it to account for the $22 \mu\text{m}$ flux density with respect to the $24 \mu\text{m}$ flux density if it were at $z = 6.5$. One could imagine that varying the AGN template could allow for the mid-infrared photometry here to be fit, but given that the $z = 1.7$ fit using typical mid-infrared templates agrees with the parameters derived from the optical/near-infrared fits, we find the $z = 6.5$ interpretation for JD2 substantially weakened.

3.2. The Optical/Near-Infrared Photometry

Given the derived redshift based on the mid-infrared photometry of the source, we critically investigate the optical/near-infrared photometry to assess potential sources of error.

The ACS *BVIz* photometric measurements are very important to the interpretation of JD2, since a significant optical detection would almost certainly rule out the $z \approx 6.5$ hypothesis. We note that Mobasher et al. (2005) erroneously reported that their ACS photometry was measured in an $0.9''$ diameter aperture, when in fact a smaller, $0.48''$ diameter aperture was used (M. Dickinson 2006, private communication). A larger aperture size would lead to more conservative photometric limits, and is probably to be recommended, given the size of the galaxy as measured from the NICMOS *H*-band images (measured half-light radius $0.3''$, uncorrected for PSF effects; see Mobasher et al.). However, a larger aperture risks including light from three faint, neighboring galaxies located about $1''$ away from JD2. We have masked out regions with diameter $0.9''$ around those three galaxies⁸ before measuring photometry for JD2 in a $1.0''$ diameter circular aperture.

The ACS images were drizzled using a point kernel (see Beckwith et al. 2006), which should lead to noise that is uncorrelated between adjacent pixels. We verified that this is the case by measuring the autocorrelation function of the noise after masking galaxies. We measured the noise on various scales, including 50 pixel apertures, as used by Beckwith et al. (2006). Our most conservative (largest) noise measurements are 31% – 37% smaller than those reported by Beckwith et al. (2006; their Table 5).

Dunlop et al. (2007) report faint detections of positive flux in the ACS *V*, *i*, and *z* bands, which, taken together, drive their photometric redshift estimate to favor a lower value, $z \approx 2.15$. We do not reproduce these measurements; using a $1.0''$ diameter aperture and our noise measurements, and the correction of ~ 0.1 mag for the energy falling outside the aperture reported in Sirianni et al. (2005; their Table 3), we find the 2σ photometric limits given in Table 2. These are ~ 0.8 mag brighter than the limits reported in Mobasher et al. (2005), mainly due to the larger aperture adopted here. It is possible that the positive flux detected in the Dunlop et al. measurements arises in part from the faint neighboring galaxies.

The NICMOS J_{110} photometry and H_{160} photometry in Mobasher et al. (2005) are very similar to those in the UDF catalog of Thompson et al. (2005). As a result, we have not remeasured these values. However, we note that the photometric values in

⁸ In another typographical error, Mobasher et al. (2005) reported masking regions $0.5''$ in diameter around the neighboring galaxies. In fact, the masking diameter was $0.9''$, which we also adopt here.

TABLE 2
REVISED OPTICAL/NEAR-INFRARED PHOTOMETRY FOR JD2

Wavelength	Photometry ^a (AB mag)
<i>B</i>	>29.7
<i>V</i>	>30.1
<i>i</i>	>30.0
<i>z</i>	>29.3
J_{110}	26.8 ± 0.3
H_{160}	24.82 ± 0.07
K_s	23.95 ± 0.132
$3.6 \mu\text{m}$	22.29 ± 0.15
$4.5 \mu\text{m}$	22.05 ± 0.15
$5.8 \mu\text{m}$	21.67 ± 0.15
$8.0 \mu\text{m}$	21.54 ± 0.15
$16 \mu\text{m}$	$21.04^{+2.86}_{-0.76}$
$22 \mu\text{m}$	19.53 ± 0.21
$24 \mu\text{m}$	19.63 ± 0.21

^a Photometric limits, where provided, are 2σ . See text for details.

Mobasher et al. (2005) do not include the NICMOS count-rate-dependent nonlinearity correction discussed in de Jong et al. (2006). The effect of this nonlinearity correction is to make the photometry brighter by 0.22 mag in the J_{110} band and 0.12 mag in the H_{160} band, as shown in Table 2.

We also remeasured the photometry of the source at IRAC wavelengths. We used SExtractor catalogs and measured the photometry in $3''$ diameter beams, similar to Mobasher et al. (2005). To derive aperture corrections and systematic uncertainties, we adopt a different approach. The primary systematic uncertainty in this measurement is the uncertain sky level due to the bright galaxy $7''$ to the southeast. We input an artificial point source whose brightness is that of JD2 into the final mosaic. The centroid of the source with respect to the bright galaxy is kept similar to that of JD2, i.e., the artificial source has a centroid that is between $7''$ and $8''$ from the galaxy. The SExtractor routine was run on this fake image and the photometry of the fake source measured. We find a systematic uncertainty whereby the extracted flux of the fake source in the catalog was brighter at 3.6 and $4.5 \mu\text{m}$ but fainter at 5.8 and $8.0 \mu\text{m}$. The process was repeated 100 times to measure the average systematic and statistical error using the corresponding point-spread function at each of the four IRAC wavelengths. We revise the aperture-corrected magnitudes for JD2 to 22.24 , 22.00 , 21.63 , and 21.51 AB magnitude at 3.6 , 4.5 , 5.8 , and $8.0 \mu\text{m}$, respectively. There is, however, a correction to be applied to these magnitudes.

There are three faint galaxies within $1''$ of JD2. Two of these are rather faint and blue, while the brightest of the three falls within the IRAC $3''$ beam. These galaxies are detected at all wavelengths between the *B* and H_{160} band. To estimate the contribution of these sources to the photometry within the IRAC beam, we fit Bruzual & Charlot (2003, hereafter BC03) templates to the multiband photometry of these sources, leaving redshift as a free parameter. We use the best-fit SEDs to estimate the redshift and corresponding flux densities at the IRAC wavelengths. We find the brightest of these three sources, located at $3^{\text{h}}32^{\text{m}}38.76^{\text{s}}$, $-27^{\circ}48'28.91''$ (J2000.0), to be at redshift 3.4 with magnitudes of 25.95 , 25.83 , 25.82 , and 25.80 at 3.6 , 4.5 , 5.8 , and $8.0 \mu\text{m}$, respectively. The second source, located at $3^{\text{h}}32^{\text{m}}38.81^{\text{s}}$, $-27^{\circ}48'39.79''$, is at $z \sim 3.1$ with a contribution that is about 0.6 mag fainter at each of the four passbands. We subtracted the contribution of both these sources from the photometry of JD2.

TABLE 3
 $z = 1.7$ SED FITS TO OPTICAL-NEAR-INFRARED PHOTOMETRY

Mass (M_{\odot})	A_V (mag)	Age (Myr)	τ (Myr)	UV SFR ($M_{\odot} \text{ yr}^{-1}$)	Corrected SFR ($M_{\odot} \text{ yr}^{-1}$)	χ^2 ^a	Notes
6.3×10^{10} *	3.6*	570*	30*	1.7×10^{-4} *	0.74*	2.4*	Photometry from Table 2; solar metallicity (BC03)*
9.8×10^{10}	4.7	400	0	8×10^{-5}	5	3.9	Mobasher et al. photometry; solar metallicity (BC03)
1.3×10^{11}	4.6	1020	30	4×10^{-5}	1.8	4.0	Mobasher et al. photometry; 0.2 solar metallicity (BC03)
4.6×10^{10}	4.3	453	700	0.003	93	1.6	Dunlop et al. photometry; solar metallicity (BC03)
1.9×10^{10}	4.7	47.5	50	0.005	308	1.6	Dunlop et al. photometry; 0.2 solar metallicity (BC03)

NOTE.—Asterisk indicates preferred fit. See § 3.3 for details.

^a Four degrees of freedom with seven data points and three parameters (age, extinction, and τ) for the Mobasher et al. (2005) photometry. The Dunlop et al. (2007) photometry has 10 data points.

To summarize, the corrected limits for JD2 in the ACS bands are about 0.8 mag brighter due to the larger aperture, the photometry in the NICMOS J_{110} and H_{160} bands is brighter by $\sim 10\%$ – 20% due to the nonlinearity correction, and the photometry in the IRAC bands is about 10% fainter on average than those adopted in Mobasher et al. (2005). The net effect is to reduce the amplitude of the apparent near-infrared to IRAC “break” slightly. The optical/near-infrared photometry of JD2 after these corrections have been applied is shown in Table 2, and for which we fit in § 3.3. For the sake of completeness, we also investigate redshift-constrained fits to the Dunlop et al. (2007) and Mobasher et al. (2005) optical/near-infrared photometry.

In addition, we attempted to fit elliptical isophotes to the galaxy to the southeast and subtracted it out from the image. This process left significant residuals due to the asymmetric nature of the *Spitzer* IRAC point-spread function. The aperture-corrected point-source photometry we measure for JD2 in images with the galaxy subtracted is 22.36, 21.95, 21.72, and 21.64 AB magnitude. The difference between these values and those quoted in Table 2 can be attributed almost entirely to the difficulty in measuring the absolute sky background. Thus, we provide photometric uncertainties of 0.15 mag for all four bands.

3.3. Revisiting the Optical/Near-Infrared Photometric Fits

We first evaluate the quality of the fits to the optical/near-infrared photometry at $z = 0.6$ using the BC03 population synthesis models. The range of parameter space for the models was solar and 0.2 solar metallicity, 19 e -folding timescales (τ) for the starburst from an instantaneous starburst to constant star formation, ages (t) from 0.1 Myr to the age of the universe at the chosen redshift, and extinction (A_V) between 0 and 10 mag. At $z = 0.6$, the $8 \mu\text{m}$ flux density is affected by dust emission and is ignored in the fits.

If JD2 is a $z = 0.6$ starburst like NGC 6240 but with silicate absorption that suppresses the observed $16 \mu\text{m}$ flux density, the weakness/nondetection of the source in the *BVIz* passbands requires $A_V = 9.9$ mag of visual extinction irrespective of whether we adopt the Dunlop et al. (2007) or Mobasher et al. (2005) photometry. This is not impossible but unusually large. It would imply a young 8 Myr old starburst with a mass of $2 \times 10^9 M_{\odot}$ and a true star formation rate, as derived from extinction correction of the ultraviolet flux, of $\sim 100 M_{\odot} \text{ yr}^{-1}$, all of which is dust obscured. The fits to the mid-infrared photometry at $z = 0.6$ imply a much lower dust-obscured star formation rate of $\sim 5 M_{\odot} \text{ yr}^{-1}$. Although it is possible for optically thick star formation, such as that found in local ultraluminous infrared galaxies (ULIRGs), to result in the mid- and far-infrared luminosity of galaxies exceeding their extinction-corrected ultraviolet luminosity, the converse is rarely true. This weakens the possibility of a $z = 0.6$ starburst.

If the source is a $z = 0.6$ obscured AGN like Mrk 231, then the contribution of the hot dust around the AGN to the near-infrared photometry needs to be subtracted before fitting. For the Mrk 231 template, we find this to be 0.8, 1.2, 1.4, 2.6, 3.5, 5.6, and $10.5 \mu\text{Jy}$ at 1.2, 1.6, 2.2, 3.6, 4.5, 5.8, and $8.0 \mu\text{m}$, respectively. The photometry at 1.1 and $1.6 \mu\text{m}$ of the source is a factor of 3–10 below the expected values, again indicating that a Mrk 231 type source, while consistent with the mid-infrared photometry, cannot fit the entire SED.

Thus, a $z = 1.7$ dusty star-forming galaxy SED is most consistent with all the photometry. We adopt this redshift and refit the optical/near-infrared data using the BC03 models. Results are shown in Table 3. HUDF-JD2 is best fit with a solar metallicity template from the BC03 library with $A_V \sim 4$ mag of visual extinction using a Calzetti (2001) dust extinction law. We caution that the metallicity is not strongly constrained. The best-fit model is a poststarburst BC03 SED with $t = 570$ Myr, $\tau = 30$ Myr, and a stellar mass of $6 \times 10^{10} M_{\odot}$. This is similar to the $z \sim 2.5$ fits presented in Mobasher et al. (2005). The result is not surprising, since poststarburst galaxies could have significant dust content from dust produced in supernovae and asymptotic giant branch stars. In fact, it has been observationally shown that the host galaxies of core-collapse and Type Ia supernovae are dustier than field galaxies with the same observed optical brightness (Chary et al. 2005). We caution, however, that the poststarburst hypothesis, motivated by the large value of t/τ , would be weakened if most of the star formation takes place in optically thick regions of the galaxy.

From the SED fits, we estimate that the star formation rate, as measured by the 1500 \AA flux escaping the galaxy, is very small ($\sim 2 \times 10^{-4} M_{\odot} \text{ yr}^{-1}$). Application of an extinction correction to the ultraviolet luminosity results in a star formation rate of $< 1 M_{\odot} \text{ yr}^{-1}$. In contrast, its true star formation rate as derived from the mid-infrared fits is ~ 80 – $90 M_{\odot} \text{ yr}^{-1}$. The fact that JD2 is a compact near-infrared source with a scale length of $\sim 0.3''$, combined with the large ratio of infrared-to-ultraviolet star formation rate estimates, strongly suggests that JD2 is being powered by a compact, optically thick starburst in its nucleus.

There is a caveat. If we use the BC03 models to solve for an independent redshift from the optical/near-infrared photometry presented in this paper, we continue to get a high-redshift minimum at $z = 7.2$, which has a reduced χ^2 of 1.05 compared to the reduced χ^2 values of 1.9 and 2.4 at $z = 2.4$ and $z = 1.7$, respectively. Thus, optical/near-infrared photometric redshifts continue to favor the high-redshift hypothesis, while mid-infrared photometric redshifts favor the lower redshift hypothesis. We favor the mid-infrared photometric redshifts derived here, since optical photometric redshifts for dusty galaxies have been shown to have a large scatter based on a comparison between spectroscopic

and photometric redshifts for 24 μm -detected sources in GOODS-N (Chary 2006).

A comparison of the properties of HUDF-JD2 with the massive, red galaxy population at $1.5 < z < 3$ is illustrative. Papovich et al. (2006) show that the star formation rate of galaxies scale with the stellar mass at these redshifts, and that the specific star formation rate of a dusty starburst with mass of $\sim 6 \times 10^{10} M_{\odot}$ is about $\sim 1\text{--}20 \text{ Gyr}^{-1}$. UDF-JD2, for $z \sim 1.7$, has a specific star formation rate of 1.6 Gyr^{-1} , which is consistent with the massive, dusty starbursts at these redshifts. The optical extinction derived for this galaxy is rather large, corresponding to $E(B-V) = 1.2$. Spectroscopically confirmed galaxies at these redshifts that are 24 μm detected have $E(B-V)$ values derived from their ultraviolet slopes of ~ 0.3 . This is most likely a bias, since spectroscopic confirmation requires the detection of optical/ultraviolet lines, which are preferentially detected in galaxies that are relatively transparent and have low extinction values. A better comparison is with the derived extinction values for local dusty starbursts presented in Hopkins et al. (2001). The average $E(B-V)$ to the stellar continuum for that sample at an infrared luminosity of $5 \times 10^{11} L_{\odot}$ is about 0.25. Thus, HUDF-JD2 does not appear to be dissimilar from dusty, LIRGs at $z \sim 2$. However, its derived $E(B-V)$ appears to be a factor of ~ 4 higher than other LIRG samples, consistent with its significant detection at mid-infrared wavelengths and compact morphology in the NICMOS 1.6 μm image, which suggests a compact, nuclear starburst similar to many local infrared-luminous galaxies.

JD2 is about 1.4 mag redder in observed $R-[3.6]$ colors and about 3 mag fainter at 3.6 μm than HR 10, a $z = 1.44$ spectroscopically confirmed dusty starburst (Stern et al. 2006). The predicted $\text{H}\alpha$ line flux for JD2, including the extinction in the line, is $\sim 10^{-18} \text{ ergs s}^{-1} \text{ cm}^{-2}$. This is a factor of 3 below the sensitivity of the existing observations in Mobasher et al. (2005) but should be detectable with a space-based near-infrared spectrograph.

4. CONCLUSIONS

We present new 16 and 22 μm mid-infrared photometry of the HUDF source JD2, which had tentatively been classified as a $z \sim 6.5$ massive galaxy. The mid-infrared spectral energy distribution shows a sharp increase in flux density between 16 and 22 μm , most consistent with the 7.7 μm PAH feature entering the 22 μm bandpass. Our analysis concludes that the galaxy is a star-forming, luminous infrared galaxy (LIRG) at a redshift of $z \sim 1.7$. The nondetection of the source in the UDF $BVIz$ data is due to the presence of $A_V \sim 4$ mag of dust internal to the galaxy. We have reevaluated the optical/near-infrared photometry of this source and find the stringent limits in Mobasher et al. (2005) are more consistent with the data rather than the marginal detection reported in Dunlop et al. (2007). Photometric redshift fits to the optical/near-infrared data alone continue to favor a $z > 6$ solution. However, the unusually high L_{MIR}/L_X for JD2 compared to other obscured AGNs, the large scatter in optical photometric redshift solutions for dusty galaxies, and the similarity between the multiwavelength properties of this galaxy and other dusty starbursts in the $1.5 < z < 3$ range lead us to favor the mid-infrared photometric redshift solution. The nondetection of a $z \sim 2$ LIRG in the deepest optical data taken to date strongly cautions against interpreting near-infrared dropout sources in shallower surveys as $z > 6$ galaxies.

We wish to thank Dave Frayer and Megan Eckart for useful advice. This work is based on observations made with the *Spitzer Space Telescope*, which is operated by the Jet Propulsion Laboratory, California Institute of Technology, under a NASA contract. Support for this work was provided by NASA through an award issued by JPL/Caltech.

REFERENCES

- Armus, L., et al. 2007, ApJ, 656, 148
 Beckwith, S. V. W., et al. 2006, AJ, 132, 1729
 Brandl, B., et al. 2004, ApJS, 154, 188
 Bruzual, G., & Charlot, S. 2003, MNRAS, 344, 1000 (BC03)
 Calzetti, D. 2001, PASP, 113, 1449
 Chary, R. 2006, in ASP Conf. Ser., At the Edge of the Universe, ed. J. Afonso, H. Ferguson, & R. Norris (San Francisco: ASP), submitted (astro-ph/0612736)
 Chary, R., & Elbaz, D. 2001, ApJ, 556, 562
 Chary, R., et al. 2005, ApJ, 635, 1022
 Chen, H.-W., & Marzke, R. O. 2004, ApJ, 615, 603
 Dale, D., & Helou, G. 2002, ApJ, 576, 159
 Davé, R., Finlator, K., & Oppenheimer, B. D. 2006, MNRAS, 370, 273
 de Jong, R., et al. 2006, in 2005 *HST* Calibration Workshop, ed. A. Koekemoer, P. Goudfrooij, & L. Dressel (Greenbelt: NASA), 121
 Dickinson, M., et al. 2003, in Mass of Galaxies at Low and High Redshift, ed. R. Bender & A. Renzini (Berlin: Springer), 324
 Dunlop, J., Cirasuolo, M., & McLure, R. J. 2007, MNRAS, 376, 1054
 Forster-Schreiber, N. M., et al. 2001, ApJ, 552, 544
 Frayer, D., et al. 2006, ApJ, 647, L9
 Fruchter, A. S., & Hook, R. N. 2002, PASP, 114, 144
 Hopkins, A. M., et al. 2001, AJ, 122, 288
 Houck, J., et al. 2004, ApJS, 154, 18
 Krabbe, A., Boeker, T., & Maiolino, R. 2001, ApJ, 557, 626
 Le Floc'h, E., et al. 2001, A&A, 367, 487
 Mobasher, B., et al. 2005, ApJ, 635, 832
 Papovich, C., et al. 2006, ApJ, 640, 92
 Sirianni, M., et al. 2005, PASP, 117, 1049
 Stern, D., Chary, R., Eisenhardt, P., & Moustakas, L. 2006, AJ, 132, 1405
 Teplitz, H. I., et al. 2006, BAAS, 209, 132.03
 Thompson, R. I., et al. 2005, AJ, 130, 1
 Yan, H., et al. 2004, ApJ, 616, 63
 Yun, M. S., Reddy, N. A., & Condon, J. 2001, ApJ, 554, 803